Jurnal Dinamis (*Scientific Journal of Mechanical Engineering*)
Journal homepage: https://talenta.usu.ac.id/dinamis/

Structural Strength Simulation of an Archimedes Screw Turbine Casing for MicroHydropower Applications

Tri Imam Sugatra[1], Suherman*[2]
[1]*Department of Mechanical Engineering Universitas Muhammadiyah Sumatera Utara 20238, Medan, Indonesia*
[2]*Department of Mechanical Engineering Universitas Muhammadiyah Sumatera Utara 20238, Medan, Indonesia*

*Corresponding Author: suherman@umsu.ac.id

ARTICLE INFO

Article history:
Received April 20th 2026
Revised May 21th 2026
Accepted June 28th 2026
Available online June 30th 2026

E-ISSN: 2809-3410

How to cite:
Tri Imam Sugatra, Paini Sri Widyawati, Suherman "Structural Strength Simulation of an Archimedes Screw Turbine Casing for MicroHydropower Applications", *Junal Dinamis (Scientific Journal of Mechanical Engineering)*, Vol. 14, No. 1, pp. 54-70, June 2026.

http://doi.org/10.32734/dinamis.v14i1.25283

ABSTRACT

The Archimedes screw turbine (AST) has emerged as a promising technology for low-head micro-hydropower generation due to its simple configuration, high operational efficiency, and environmental compatibility. Nevertheless, studies addressing the structural performance and mechanical reliability of AST casing systems remain limited, particularly under different static loading conditions. This study aims to evaluate the structural strength of an ASTM A36 steel casing for an Archimedes screw turbine using finite element analysis in SolidWorks 2020. The novelty of this research lies in the integrated structural assessment of a closed-type AST casing, analysing stress distribution, strain behaviour, displacement characteristics, and factor of safety under various loading conditions prior to practical implementation. Static loads of 55.154 N, 57.704 N, and 84.584 N were applied to the casing structure. The simulation results revealed that the maximum von Mises stress increased from 7.517×10^6 N/m² to 1.152×10^7 N/m² as the load increased, while the maximum displacement rose from 1.050×10^{-1} mm to 1.612×10^{-1} mm. In contrast, the factor of safety decreased from 33.26 to 21.70, although all obtained values remained below the yield strength limit of ASTM A36 steel. The highest stress and strain concentrations were identified near the casing support and end sections, indicating critical regions requiring structural attention. Overall, the proposed casing design demonstrates satisfactory mechanical performance and structural safety for low-head micro-hydropower applications employing Archimedes screw turbines.

Keyword: *Archimedes screw turbine, Casing AST turbine, Solidworks*

ABSTRAK

Turbin sekrup Archimedes (AST) telah muncul sebagai teknologi yang menjanjikan untuk pembangkit listrik mikro-hidro berdaya rendah karena konfigurasinya yang sederhana, efisiensi operasional yang tinggi, dan kompatibilitas lingkungan. Namun demikian, studi yang membahas kinerja struktural dan keandalan mekanis sistem selubung AST masih terbatas, terutama di bawah kondisi pembebanan statis yang berbeda. Studi ini bertujuan untuk mengevaluasi kekuatan struktural selubung baja ASTM A36 yang dirancang untuk turbin sekrup Archimedes melalui analisis elemen hingga menggunakan SolidWorks 2020. Kebaruan penelitian ini terletak pada penilaian struktural terintegrasi dari selubung AST tipe tertutup dengan menganalisis distribusi tegangan, perilaku regangan, karakteristik perpindahan, dan faktor keamanan di bawah beberapa variasi pembebanan sebelum implementasi praktis. Beban statis sebesar 55,154 N, 57,704 N, dan 84,584 N diterapkan pada struktur selubung. Hasil simulasi menunjukkan bahwa tegangan von Mises maksimum meningkat dari $7,517 \times 10^6$ N/m² menjadi $1,152 \times 10^7$ N/m² seiring peningkatan beban, sedangkan perpindahan maksimum meningkat dari $1,050 \times 10^{-1}$ mm menjadi $1,612 \times 10^{-1}$ mm. Sebaliknya, faktor keamanan menurun dari 33,26 menjadi 21,70, meskipun semua nilai yang diperoleh tetap di bawah batas kekuatan luluh baja ASTM A36. Konsentrasi tegangan dan regangan tertinggi diidentifikasi di dekat penyangga selubung dan bagian ujung, menunjukkan daerah kritis yang

membutuhkan perhatian struktural. Secara keseluruhan, desain selubung yang diusulkan menunjukkan kinerja mekanis dan keamanan struktural yang memuaskan untuk aplikasi pembangkit listrik mikro-hidro berdaya rendah yang menggunakan turbin sekrup Archimedes.
.

Kata kunci: Turbin screw Archimedes, Casing turbin AST, Solidworks

1. Introduction

Electricity is the primary source of energy in modern life and is generated by various power plants, including hydroelectric, gas turbine, steam, diesel, and nuclear power plants. In Indonesia, electricity demand is still predominantly met by fossil fuels such as petroleum and coal, which have negative environmental impacts due to CO_2 emissions [1]. Therefore, the utilisation of renewable energy has become increasingly important, one of which is through the potential of water resources such as rivers and irrigation canals [2]. Indonesia has significant hydropower potential; however, it has not been utilised optimally due to limitations in turbine technology, particularly at low-head conditions. At present, Pelton, Francis, Kaplan, and Crossflow turbines are still commonly used for medium to high head applications [3]. River and irrigation flows can be utilised for micro-hydropower plants. One of the turbines employed is the Archimedes screw turbine, which operates as the reverse of a screw pump, utilising low-head water flow to rotate the turbine and generate electricity through a generator [4]. The Archimedes screw pump is one of the oldest pumps still in use today due to its advantages, with optimal performance achieved at an installation angle of 30°–40° [5].

Micro-hydropower is a small-scale hydroelectric power generation system that utilises the flow of rivers, irrigation channels, or waterfalls [6]. This system consists of water, a turbine, and a generator, and operates by harnessing potential energy arising from differences in elevation (head) to produce electricity. The principle of micro-hydropower (PLTMH) is to utilise water flow and elevation differences to drive the turbine, generating mechanical energy which is then converted into electrical energy by a generator [7]. A water turbine is a hydraulic turbine that utilises the flow of water, consisting of a shaft, fixed blades to direct the flow, and rotating blades to generate rotational force. Turbines are classified based on head and flow rate into impulse and reaction turbines [8]. Hydropower turbines are classified into two types: impulse and reaction. Impulse turbines convert potential energy into kinetic energy through a nozzle (e.g. Pelton, Turgo, and Crossflow), whereas reaction turbines utilise pressure differences across the blades to rotate the runner (e.g. Francis and Kaplan) [9]. The Archimedes screw is an ancient machine for lifting water that remains in use today. It consists of a helical surface wrapped around a cylindrical shaft and can also function as a turbine under low-head conditions. Operating on the reverse principle of a pump, the flow of water rotates the screw, thereby generating electrical energy efficiently [9].

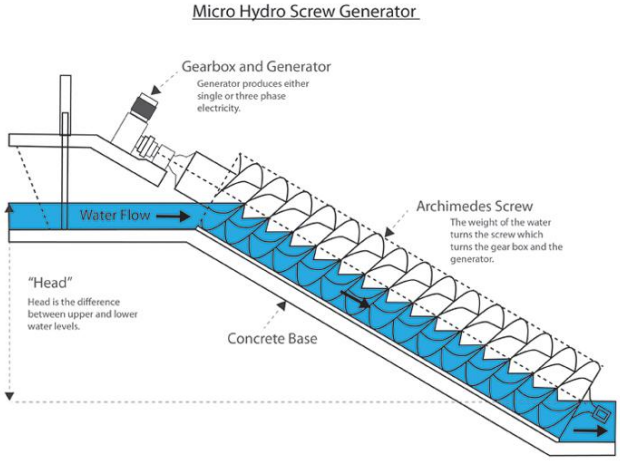

Figure 1. Schematic AST Turbine [10]

According to Havendri and Lius [11], the Archimedes screw turbine is particularly advantageous for large flow rates under low-head conditions. It features a simple design, is environmentally friendly, does not require a draft tube, operates efficiently across a range of flow rates, and requires minimal maintenance. The blade plays a crucial role in water interaction. This turbine consists of two types: the steel trough (open) type and the closed compact (enclosed) type.

(a) (b)

Figure 2. Screw Turbine: (a) Steel Trough Type and (b) Closed Compact Installation Type

In recent years, significant progress has been achieved in improving the design and performance of Archimedes Screw Turbines (ASTs) through numerical and computational approaches. Simulation tools such as SolidWorks and ANSYS have been widely utilised to evaluate turbine behaviour under various operating conditions [12-14]. These approaches enable detailed analyses of fluid behaviour, hydraulic performance, and structural characteristics, thereby reducing experimental costs and accelerating design optimisation processes.

Previous studies on ASTs have predominantly focused on fluid dynamics and performance optimisation. Brinas, et al. [15], for example, performed a numerical simulation of a dual AST system using SolidWorks Flow Simulation and provided detailed information regarding flow trajectories, fluid velocity, pressure distribution, temperature characteristics, and leakage behaviour. Furthermore, several researchers have investigated the effects of geometrical parameters on turbine performance. Chan, et al. [12] reported that the inclination angle significantly affects rotational speed, torque, and overall efficiency. Similarly, parameters such as blade number, blade curvature angle, blade pitch angle, and turbine inclination angle have been shown to influence torque generation and system performance [16, 17]. In addition, important design variables such as outer radius, pitch, and the number of pitches can be optimised through simulation-based approaches [18]. Abd Rahim, et al. [19] further demonstrated that discrepancies may exist between numerical and experimental findings, with simulation results indicating an optimum inclination angle of 25° and experimental results suggesting an optimum value of 38°.

In addition to hydraulic and performance studies, structural analyses have been conducted to evaluate the mechanical behaviour of turbine components. Andi Saidah [20] investigated stress and strain distributions in screw blades to understand the structural response under loading conditions. However, these structural investigations have primarily concentrated on rotating components, particularly the blades, while limited attention has been given to other supporting structures, especially the turbine casing.

The turbine casing plays an essential role beyond functioning as a protective enclosure. It acts as a load-bearing component, maintaining structural integrity, supporting component alignment, and withstanding forces from water pressure and turbine operation. Inadequate casing strength may result in excessive deformation, localised stress concentrations, and structural instability, ultimately reducing system efficiency and operational reliability. Such conditions may become increasingly critical during long-term operation in micro-hydropower systems where the turbine is continuously subjected to mechanical loading.

Despite the considerable number of studies on AST performance and blade behaviour, a clear research gap remains in the structural assessment of turbine casing components. Existing investigations have focused predominantly on hydraulic performance and blade-related characteristics, whereas comprehensive studies of the casing's mechanical integrity remain limited. Consequently, the structural reliability of the casing under operational loading conditions is not well understood.

Therefore, this study aims to address this gap by investigating the structural integrity of the Archimedes screw turbine casing under loading conditions using Finite Element Analysis (FEA) in SolidWorks Simulation. Unlike previous studies that mainly focused on fluid dynamics and turbine performance optimisation, this work evaluates stress distribution, strain characteristics, displacement behaviour, and factor of safety within the casing structure. The findings are expected to provide a better understanding of the mechanical reliability of AST casing systems and to contribute to the development of safer, more durable turbine designs for long-term micro-hydropower applications.

2. Methods

2.1. AST Turbine Design

In this study, SolidWorks 2020 software was used to design the AST turbine, as presented in Figure 3.

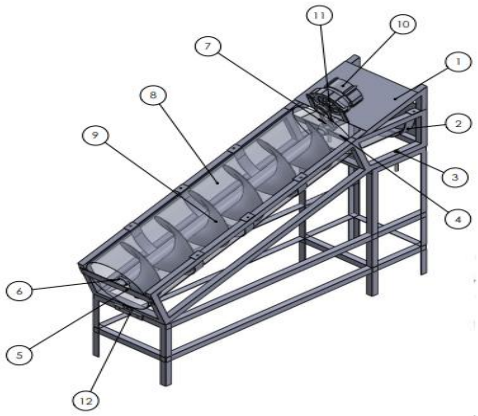

1. Chassis
2. Holder Cover Turbine
3. Bolt Adjuster
4. Holder Turbine
5. Holder Turbine
6. Bearing
7. Pulley
8. Turbine Casing
9. Turbine
10. Alternator
11. *Belt*
12. *Hinge*

Figure 3**.** Design of Archimedes Screw Turbine.

Table 1 Specification of Archimedes Screw Turbine

Parameters	Value
Inclination Angle	30°
Outer Diameter screw	302 mm
Outer Diameter Casing	306 mm
Thickness of Screw	2 mm
Pitch of Screw	180 mm
High of Screw	100 mm
Blade of Screw	1
Number of Screw	6
Diameter axle	25 mm
Length axle	1220 mm
Length frame	1488 mm
High frame	1100 mm
Width frame	450 mm

2.2. Materials Selection

Prior to conducting the simulation, material selection was performed. The material used in this study is ASTM A36 mild steel plate. ASTM A36 carbon steel is a general low-carbon steel, with a carbon content of less than 0.3%, making it very ductile and suitable for forming, machining, and welding. Heat treatment has only a minimal effect on ASTM A36 steel. This steel also contains several alloying elements, including manganese, sulphur, phosphorus, and silicon. The mechanical properties of ASTM A36 steel are presented in Table 2.

Table 2: Properties of Mild Steel *ASTM A36*

Property	value
Elastic Modulus (N/mm^2)	200000
Poisson ratio	0.26
Shear modulus (N/mm^2)	79300
Mass density (kg/m^3)	7850
Tensile strength (N/mm^2)	400
Yield strength (N/mm^2)	250

2.3. Screw Casing Design.

The turbine casing design and material strength simulation were performed in SolidWorks. The simulation was used to determine the stress, displacement, and Factor of Safety of the turbine casing. The turbine casing design is presented in Figure 4.

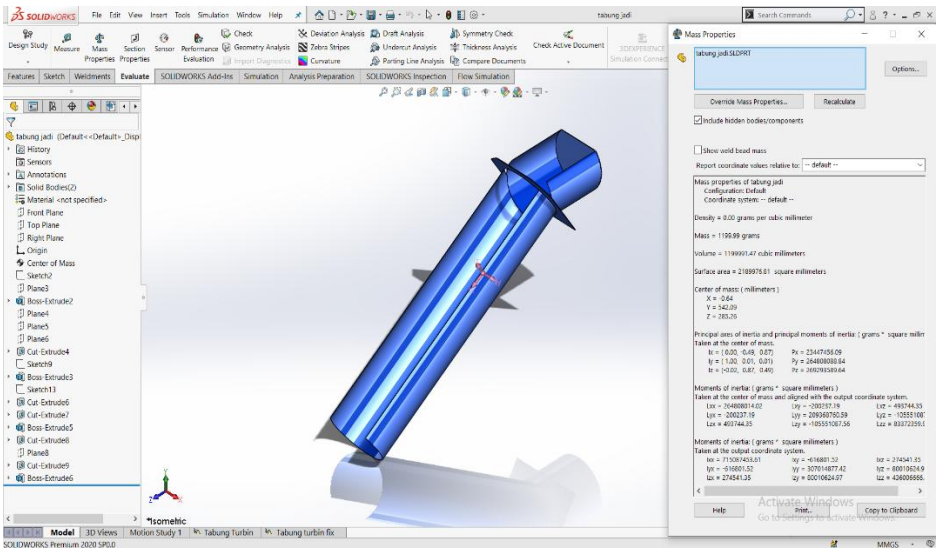

Figure 4. Design of AST turbine *Casing*.

2.4. Structural Strength Simulation of the Screw Turbine Casing

The final stage is to perform a structural strength simulation of the casing by applying loading variations to determine the resulting stress, displacement, and Factor of Safety. The structural strength simulation process consists of:

1. Selecting the material type for the designed casing as presented in Table 2
2. Selecting the area to restrain the part from movement when a load is applied. For the casing, the upper and lower base sections are selected. This process is carried out in the Fixtures section, then right-click and choose Fixed Geometry as shown in Figure 5.

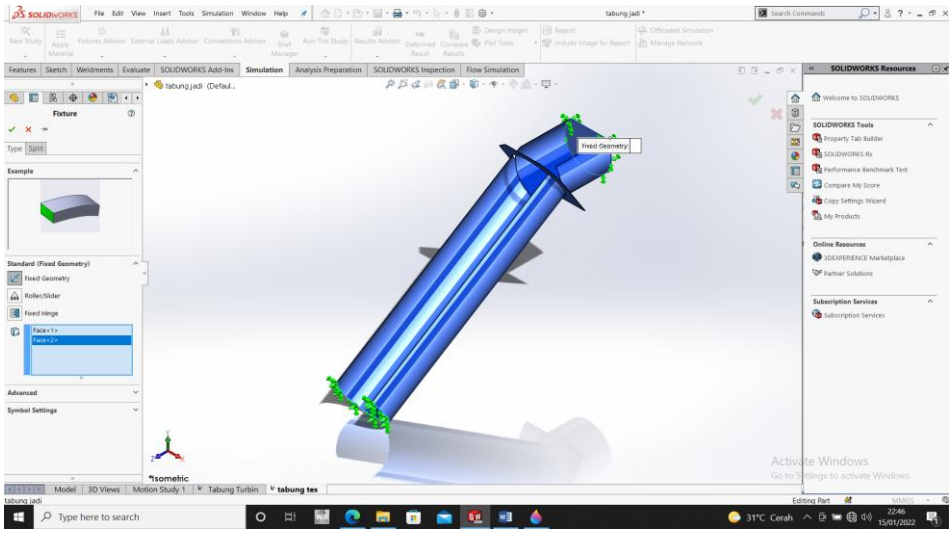

Figure 5. Selection of Support Areas on the Turbine Casing.

3. Apply force or loading via the External Loads menu, then right-click and select Force. The loading area is located in the upper and middle sections (Figure 6)

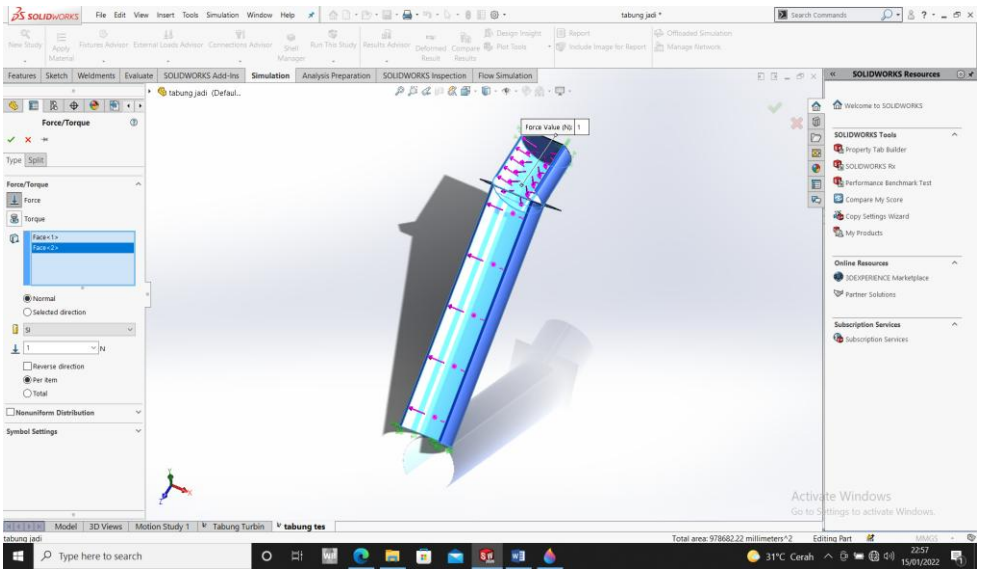

Figure 6. Input of the Applied Load.

4. Performing the meshing process via the Mesh menu, then selecting Create Mesh to initiate the meshing process. In this stage, the entire casing geometry is divided into smaller elements to approximate real conditions. This stage uses the Finite Element Method, in which the meshing process runs automatically in a few minutes (Figure 7). The duration of this process depends on the number of elements in the designed structure.

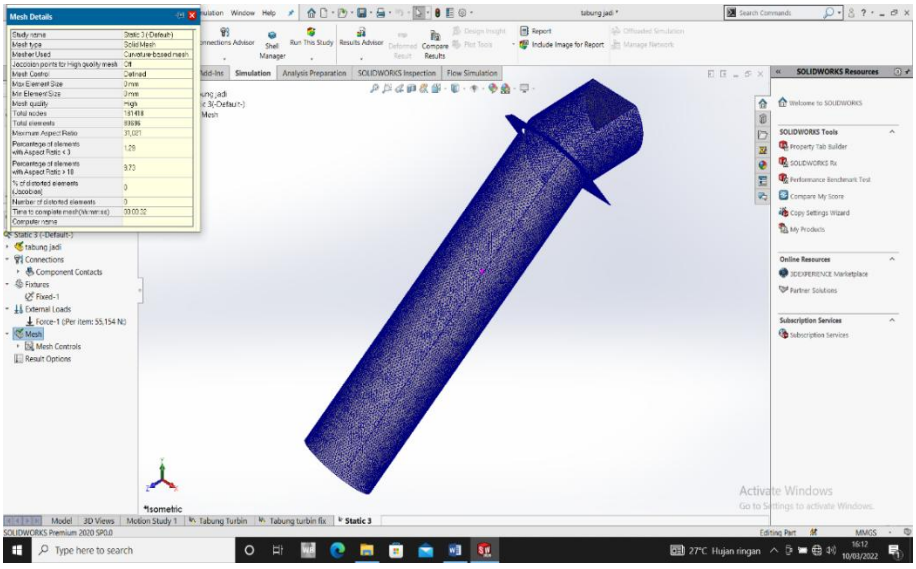

Figure 7. Meshing Process.

5. Running the 'Run This Study' command to observe the results of the structural strength simulation of the casing made of ASTM A36 mild steel. SolidWorks, with its capability to perform Finite Element Method analysis through its built-in programming, can provide simulation results including stress, displacement, strain, and Factor of Safety. The simulation results are saved using the Report feature in the Command Manager.
6. The finite element model was discretised using a curvature-based mesh with high mesh quality. The maximum and minimum element sizes were set to 7 mm and 3 mm, respectively. The mesh consisted of 15,418 nodes and 8,596 tetrahedral elements. Boundary conditions were defined by applying a fixed constraint at one end of the structure and an external force of 55.154 N to the loading region.

3. Result and Discussions

The structural strength simulation of the screw turbine casing made of ASTM A36 material was carried out under three loading variations of 55.154 N, 57.704 N, and 84.584 N. The results of the simulation can be described as follows:

Stress Distribution Analysis

Von Mises stress is a static stress calculated based on the applied loading. The material strength analysis of the screw turbine casing using SolidWorks 2020 with ASTM A36 material shows that the maximum stress is indicated by a red colour gradient, while the minimum stress is indicated by a blue colour gradient.

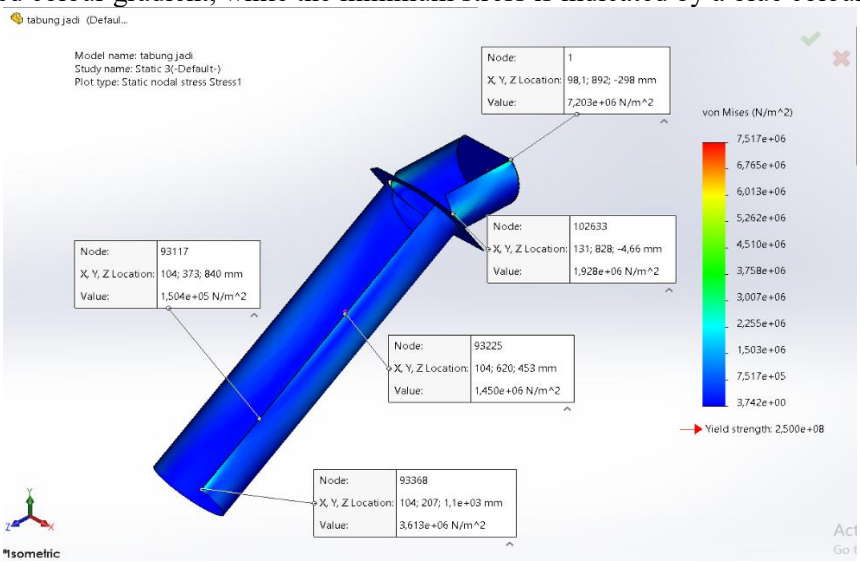

Figure 8. Stress simulation results under a load of 55.154 N.

The area of maximum stress is located at the base of the casing and at the end of the screw turbine casing. Under a load of 55.154 N, the maximum stress obtained is 7.517 × 10^6 N/m² (Figure 8). The area of minimum stress is located around the elements leading towards the end section, close to the casing support area. Meanwhile, the minimum stress obtained is 3.742 × 10 N/m² (Figure 8).

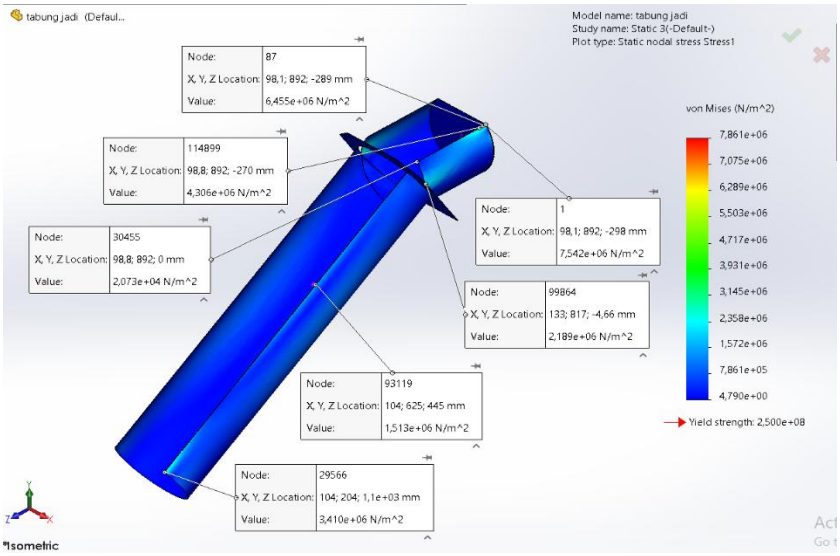

Figure 9. Stress simulation results under a load of 57.704 N

The area of maximum stress is located at the base of the casing and at the end of the screw turbine casing. Under a load of 57.704 N, the maximum stress obtained is 7.861 × 10^6 N/m² (Figure 9). The area of minimum stress is located around the elements leading towards the end section, close to the casing support area. Meanwhile, the minimum stress obtained is 4.790 × 10 N/m² (Figure 9).

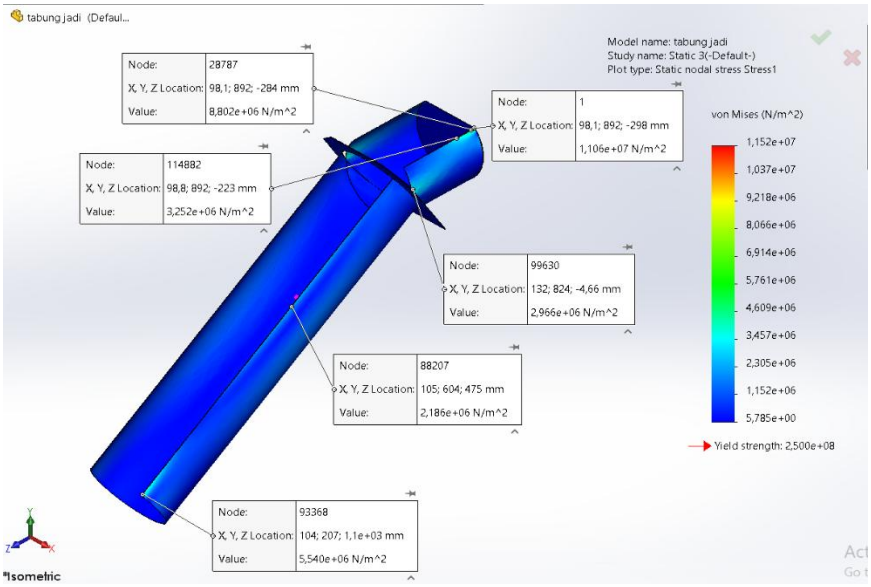

Figure 10. Stress simulation results under a load of 84.584 N

The area of maximum stress is located at the base of the casing and at the end of the screw turbine casing. Under a load of 84.584 N, the maximum stress obtained is 1.152×10^7 N/m² (Figure 10). The area of minimum stress is located around the elements leading towards the end section, close to the casing support area. Meanwhile, the minimum stress obtained is 5.785 × 10 N/m² (Figure 10).

Based on the yield strength of the mild steel used, ASTM A36 at 2.5×10^8 N/m², it can be confirmed that the design can withstand the applied load, as the maximum stress obtained does not exceed the material's yield strength.

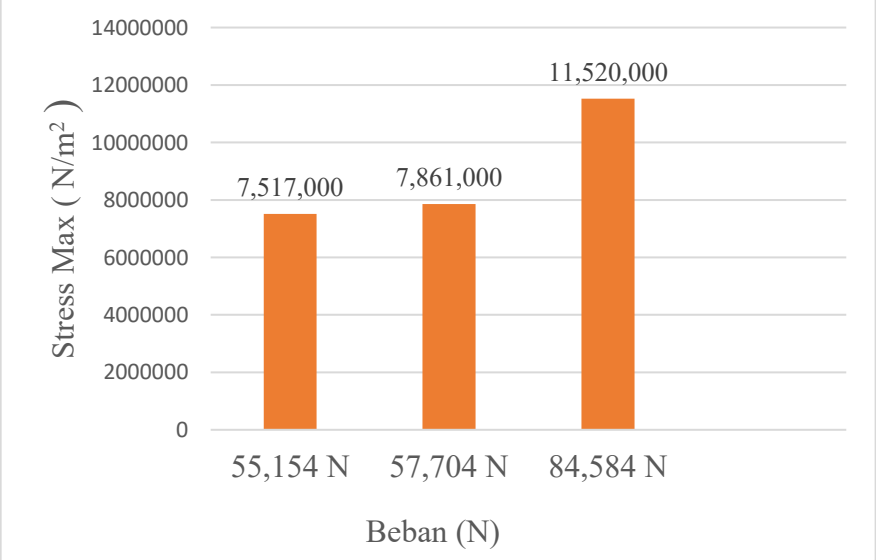

Figure 11. Graph of Maximum Stress versus Load Variation

The finite element simulation results illustrate the variation of maximum stress on the AST casing made of A36 steel under different loading conditions. As shown in the graph, the applied loads of 55,154 N, 57,704 N, and 84,584 N produce maximum stress values of approximately 7.52 MPa, 7.86 MPa, and 11.52 MPa, respectively. A clear upward trend in maximum stress is observed as the applied load increases. Between 55,154 N and 57,704 N, the stress increment is relatively small, indicating a near-linear elastic response of the material within this loading range. However, a more significant increase in stress is observed when the load reaches 84,584 N, indicating that the structure experiences higher stress concentration under higher loading conditions. Despite this increase, the maximum stress values remain substantially below the yield strength of A36 steel (approximately 250 MPa). This indicates that the casing structure operates well within the elastic region for all simulated load cases, and no plastic deformation is expected. Therefore, from a strength perspective, the AST casing demonstrates a high level of structural safety under the applied loads.

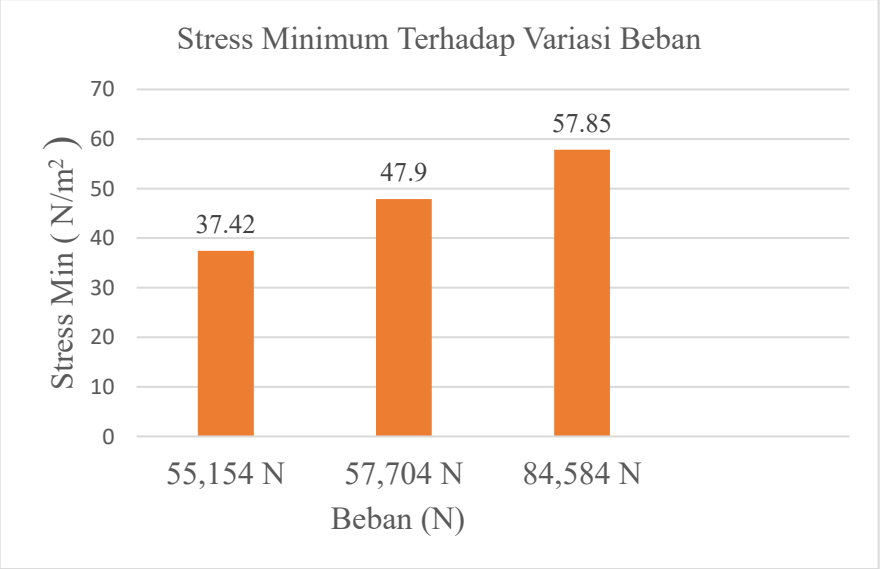

Figure 12. Minimum Stress Graph with Respect to Load Variation

The finite element simulation results indicate that the maximum von Mises stress increased with increasing applied load, demonstrating the expected mechanical response of the AST casing structure under elastic loading conditions. The highest stress values were consistently observed at the casing support and end regions, indicating localised stress concentrations.

The occurrence of stress concentrations in these regions may be attributed to abrupt geometric transitions and constrained boundary conditions that alter the load-transfer path through the structure. Such locations are generally considered critical regions because localised stresses may initiate structural failure or fatigue damage under long-term operation. Although the stress magnitude increased with applied load, the maximum stress remained significantly below the ASTM A36 yield strength (250 MPa), confirming that the structure operated within the elastic deformation region.

Compared with previous studies that primarily analysed blade stress behaviour in Archimedes screw turbines, the present study demonstrates that the casing structure exhibits similar concentration behaviour in geometrically constrained regions, although the overall stress level remains substantially below the material limit. This finding highlights the importance of evaluating casing integrity in addition to turbine blade performance.

From a design perspective, stress concentration areas near support regions could be reduced through local geometric modification, such as smoother curvature transitions or additional reinforcement features to improve load distribution.

Strain Behaviour Analysis

Strain is a component of deformation, defined as the relative change in the positions of particles within a non-rigid body. Areas experiencing maximum strain are indicated by a red colour gradient, whereas areas experiencing minimum strain are indicated by a blue colour gradient.

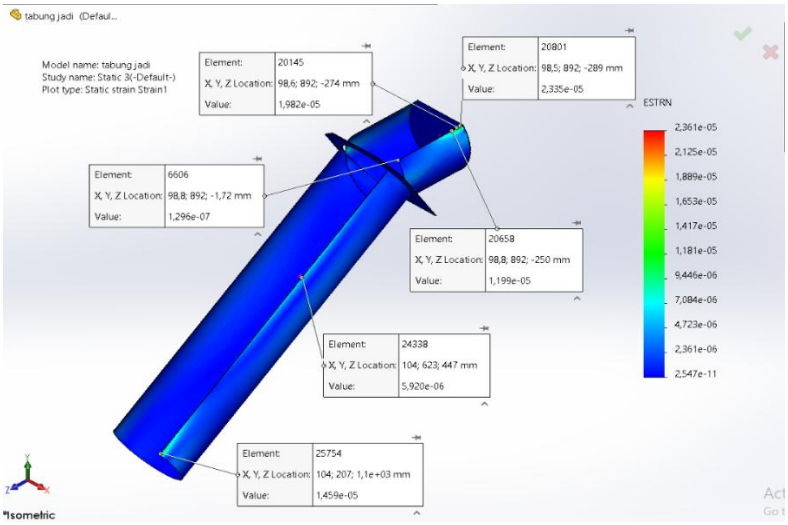

Figure 13. Results of the Strain Simulation under a Load of 55.154 N

The area of maximum strain is located at the base of the casing and at the end of the screw turbine casing. Under a load of 55.154 N, the maximum strain obtained is 2.361×10^{-5} N/m² (Figure 13). The area of minimum strain is located around the elements leading towards the end section, close to the casing support area. Meanwhile, the minimum strain obtained is 2.547×10^{-11} N/m² (Figure 13).

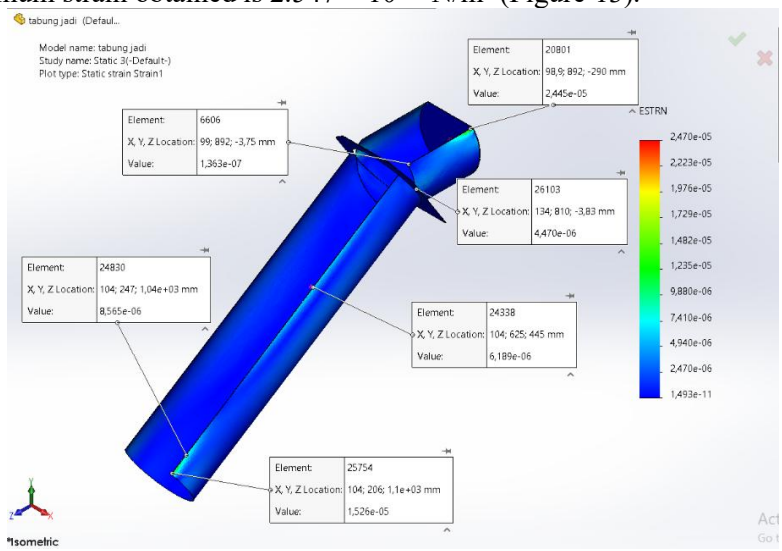

Figure 14. Results of the Strain Simulation under a Load of 57.704 N

The area of maximum strain is located at the base of the casing and at the end of the screw turbine casing. Under a load of 57.704 N, the maximum strain obtained is 2.470×10^{-5} N/m² (Figure 14). The area of minimum strain is located around the elements leading towards the end section, close to the casing support area. Meanwhile, the minimum strain obtained is 1.493×10^{-11} N/m² (Figure 14).

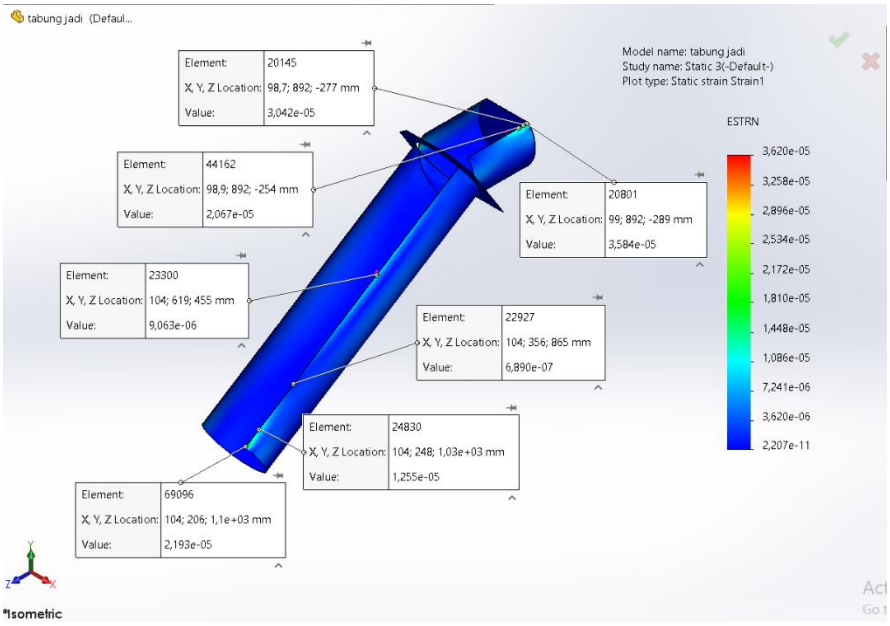

Figure 15. Results of the Strain Simulation under a Load of 84.584 N

The area of maximum strain is located at the base of the casing and at the end of the screw turbine casing. Under a load of 84.584 N, the maximum strain obtained is 3.620×10^{-5} N/m² (Figure 15). The area of minimum strain is located around the elements leading towards the end section, close to the casing support area. Meanwhile, the minimum strain obtained is 2.207×10^{-11} N/m² (Figure 15). Based on the strain analysis results, it is found that under elastic conditions, stress and strain vary proportionally, indicating that higher stress corresponds to higher strain.

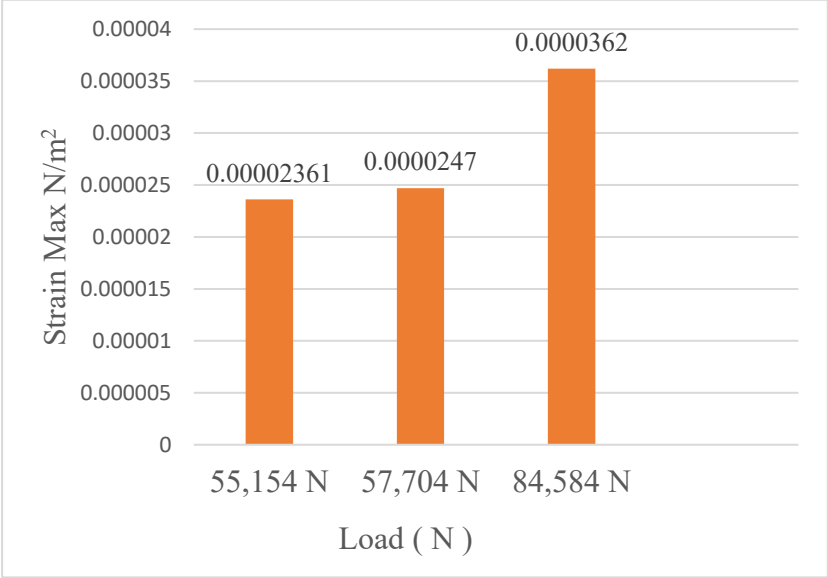

Figure 16. Maximum Strain Graph with Load Variation

The SolidWorks simulation results demonstrate that the maximum strain in the AST turbine casing increases with the applied load, indicating a consistent mechanical response (Figure 16). At 55.154 N and 57.704 N, the strain values are 2.361×10^{-5} and 2.47×10^{-5}, respectively, indicating nearly linear, stable elastic behaviour. A more pronounced increase is observed at 84.584 N, where the strain reaches 3.62×10^{-5}. This suggests a higher degree of deformation, potentially influenced by local stress concentrations. Nevertheless, the strain values remain within the elastic range, indicating no plastic deformation. Overall, the results confirm that the casing structure maintains good mechanical integrity under the applied loading conditions, although further evaluation of critical and safety factors is recommended for improved reliability.

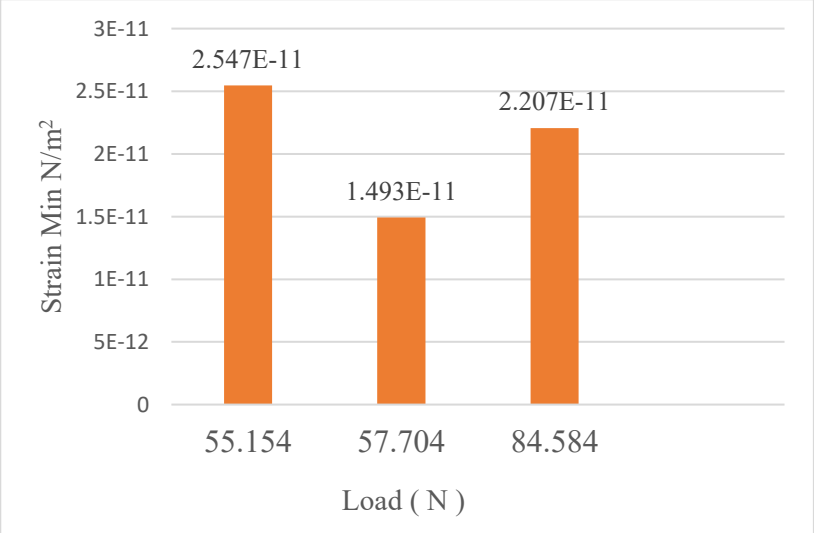

Figure 17. Minimum Strain Graph with Load Variation

The strain analysis demonstrated a proportional relationship between stress and deformation behaviour, which is consistent with Hooke's law under elastic conditions. The highest strain values were observed in regions of maximum stress concentration, particularly near the casing support and end sections.

It should be noted that strain is a dimensionless quantity and therefore does not possess units of N/m². The strain values obtained in this study indicate that the casing deformation remained within the elastic range, suggesting that no permanent deformation occurred under the investigated loading conditions.

The gradual increase in strain with increasing load confirms the casing's structural stability and indicates that the material exhibits predictable deformation behaviour. Nevertheless, repeated operational loading may introduce fatigue effects over extended periods; therefore, fatigue analysis should be considered in future investigations.

Displacement Analysis

The results of the displacement analysis are shown for the regions experiencing deformation under the applied force. Areas with maximum displacement are indicated by a red colour gradient, whereas areas with minimum displacement are indicated by a blue colour gradient.

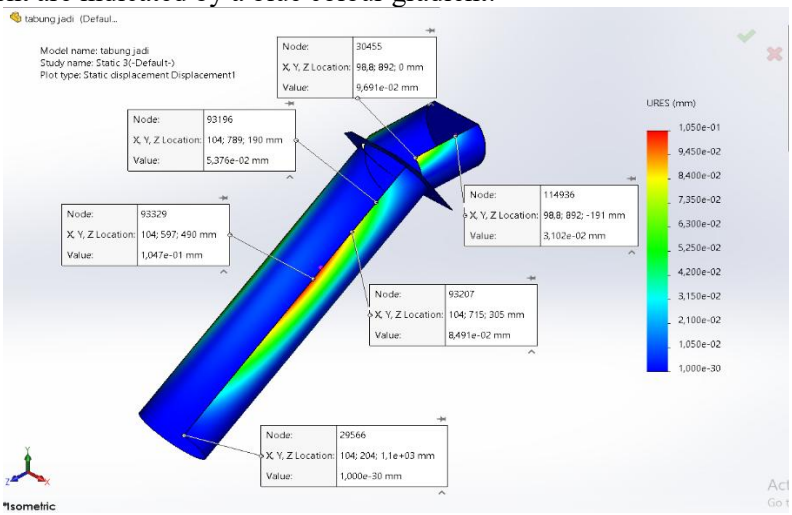

Figure 18. Results of the Displacement Simulation under a Load of 55.154 N.

Under a load of 55.154 N, the maximum displacement obtained is 1.050×10^{-1} mm (Figure 18). The area of maximum displacement under this loading is located around the edges of the screw casing. Meanwhile, the minimum displacement of the screw casing under a load of 55.154 N is 0 mm (Figure 18). The area of minimum displacement is located at the centre of the screw casing.

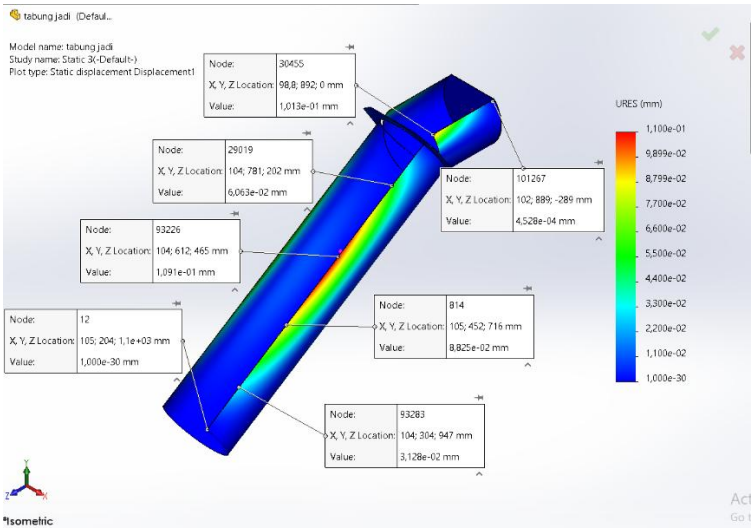

Figure 19. Results of the Displacement Simulation under a Load of 57.704 N

Under a load of 57.704 N, the maximum displacement obtained is 1.100×10^{-1} mm (Figure 19). The area of maximum displacement under this loading is located around the edges of the screw casing. Meanwhile, the minimum displacement of the screw casing under a load of 57.704 N is 0 mm (Figure 19). The area of minimum displacement is located at the centre of the screw casing.

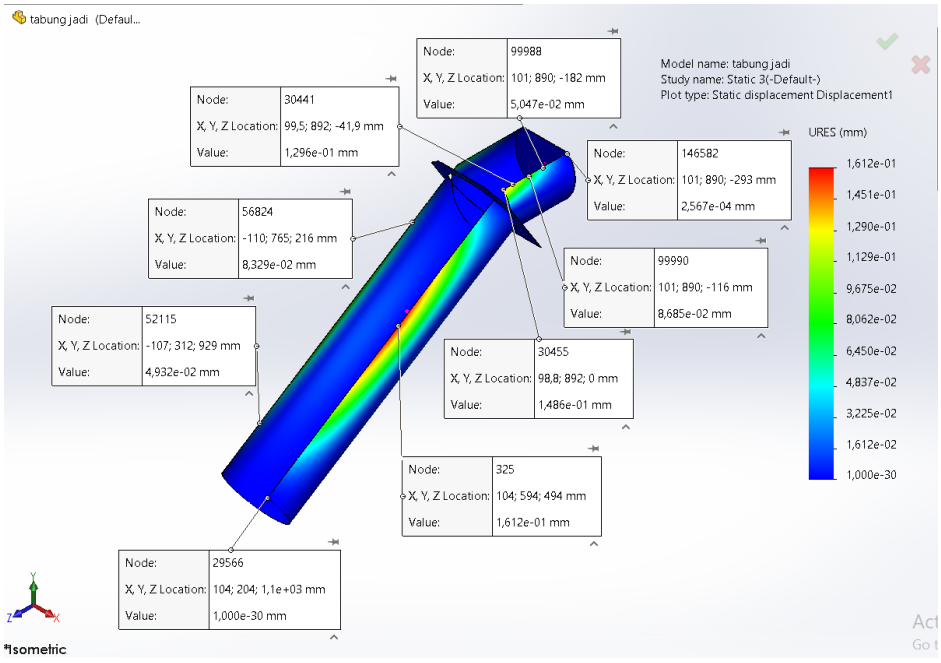

Figure 20 Results of the Displacement Simulation under a Load of 84.584 N

Under a load of 84.584 N, the maximum displacement obtained is 1.612×10^{-1} mm (Figure 20). The area of maximum displacement under this loading is located around the edges of the screw casing. Meanwhile, the minimum displacement of the screw casing under a load of 84.584 N is 0 mm (Figure 20). The area of minimum displacement is located at the centre of the screw casing.

Therefore, from the results of this displacement analysis, it can be concluded that the screw casing made of ASTM A36 material experiences varying displacements corresponding to different loading variations. This indicates that the greater the load applied to the screw casing, the greater the resulting displacement.

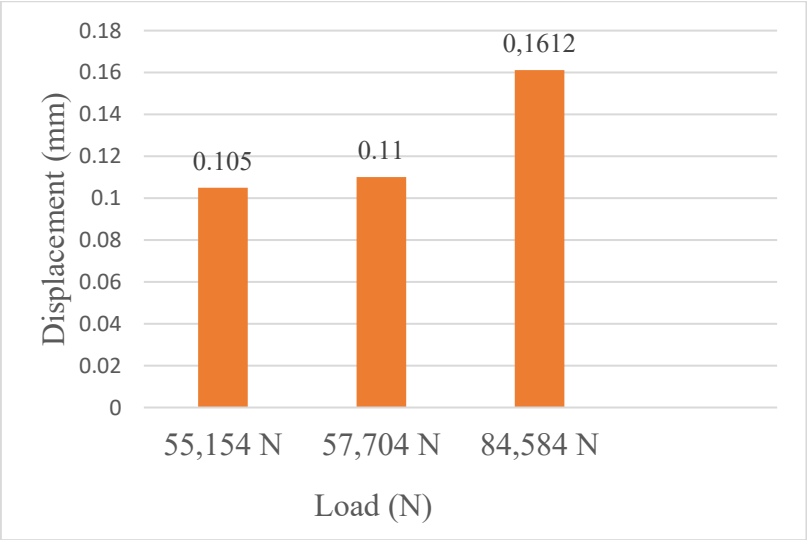

Figure 21. Displacement Graph with Load Variation

The displacement results revealed that deformation increased progressively with increasing applied load, with the maximum displacement occurring near the outer edges of the casing structure. This behaviour indicates that the unsupported regions exhibit greater flexibility than the constrained support sections.

Although displacement increased under higher loading conditions, the magnitude of deformation remained relatively small compared with the casing's overall dimensions. Consequently, no significant structural instability or excessive deflection is expected during operation.

From an engineering standpoint, minimising displacement is important because excessive deformation may affect alignment between the turbine shaft and casing assembly. Future design optimisation could therefore include increasing local stiffness in regions experiencing higher displacement.

Factor of Safety Analysis

The Factor of Safety in this plot represents the model's material strength in resisting the stresses induced by the applied load. By comparing the material's yield strength with the maximum von Mises stress, the distribution of the Factor of Safety (FOS) across the entire model can be obtained. In the FOS analysis, the colour blue indicates a very high level of design safety. Based on the analysis results, the FOS distribution is predominantly represented by areas with a red colour gradient.

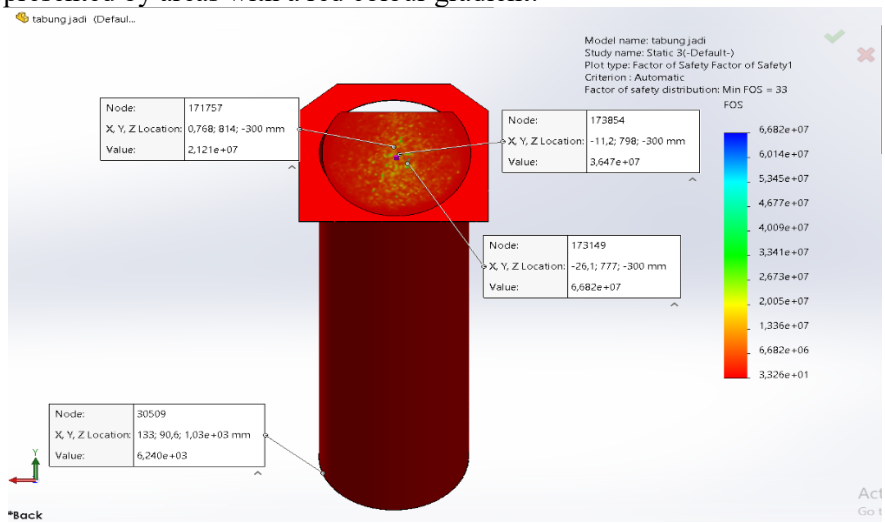

Figure 22. Results of the Factor of Safety Simulation under a Load of 55.154 N

Under a load of 55.154 N, the Factor of Safety obtained is 3.326×10^{1} (Figure 22). This safety value occurs across the entire casing subjected to the applied force. This indicates that the mild steel casing provides a good level of safety. Therefore, it can be confirmed that the screw casing made of ASTM A36 material is safe in withstanding the applied load.

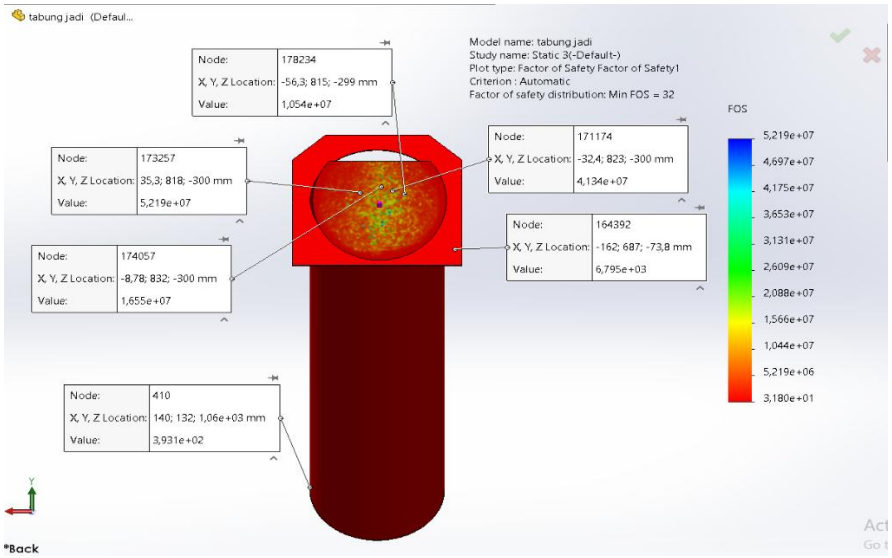

Figure 23. Results of the Factor of Safety Simulation under a Load of 57.704 N

Under a load of 57.704 N, the Factor of Safety obtained is 3.180×10^{1} (Figure 23). This safety value occurs across the entire casing subjected to the applied force. This indicates that the mild steel casing provides a good level of safety. Therefore, it can be confirmed that the screw casing made of ASTM A36 material is safe in withstanding the applied load.

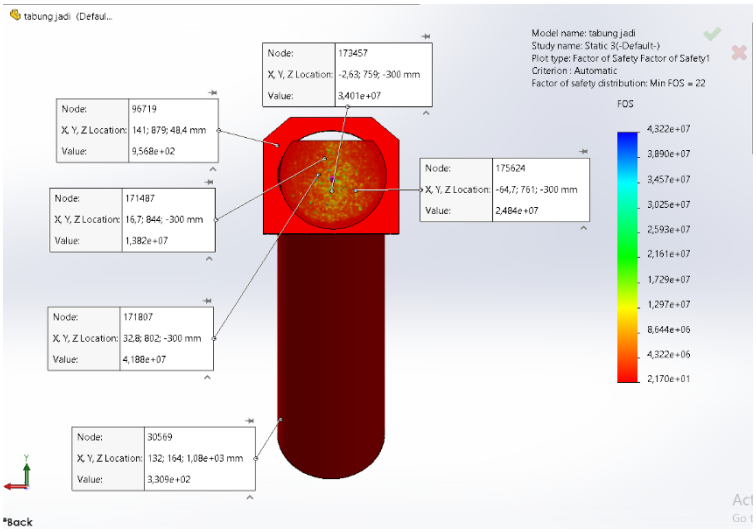

Figure 24. Results of the Factor of Safety Simulation under a Load of 84.584 N

Under a load of 84.584 N, the Factor of Safety obtained is 2.170×10^{1} (Figure 24). This safety value occurs across the entire casing subjected to the applied force. This indicates that the mild steel casing provides a good level of safety. Therefore, it can be confirmed that the screw casing made of ASTM A36 material is safe in withstanding the applied load. If the Factor of Safety is very low, the likelihood of failure becomes high, and thus the structural design is unacceptable. Failure may refer to a fracture or damage occurring within a structure. From the results of the Factor of Safety (FOS) analysis, it can be concluded that the screw casing made of ASTM A36 mild steel is considered safe to withstand a maximum load of 55.154 N. Meanwhile, the resulting FOS values indicate that as the applied load increases, the Factor of Safety decreases.

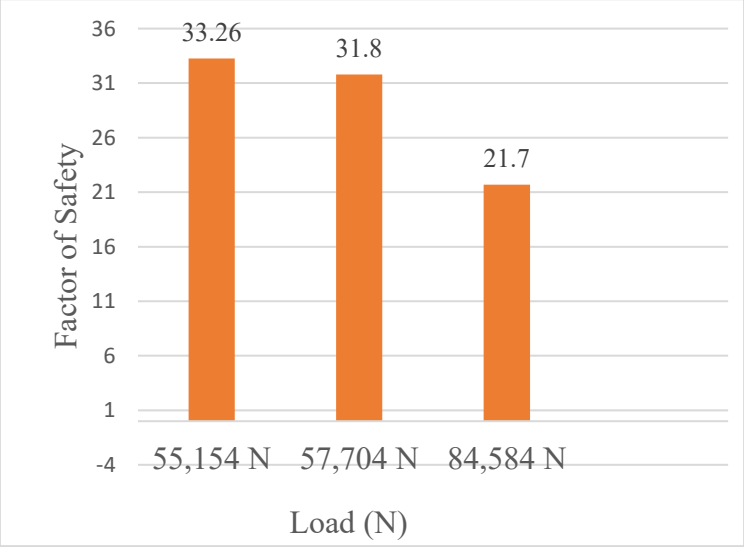

Figure 25 Graph of Factor of Safety versus Load Variation.

The Factor of Safety (FOS) analysis indicated a gradual reduction in safety margin with increasing applied load. Nevertheless, even at the highest applied load of 84.584 N, the minimum FOS remained significantly above the commonly accepted engineering safety limit.

The very high FOS values obtained in this study suggest that the casing design may exhibit characteristics of structural overdesign. While high safety margins improve reliability and reduce the probability of structural failure, excessively conservative designs may increase material usage, manufacturing cost, and overall system weight.

Therefore, optimisation of the casing geometry may be considered to reduce material consumption while maintaining adequate structural integrity. This optimisation approach could potentially improve both economic efficiency and overall system performance.

Furthermore, all simulated loading conditions demonstrated safe structural behaviour; therefore, it is inappropriate to state that the casing is only safe up to a load of 55.154 N. The simulation results indicate that the casing remained structurally safe throughout all investigated loading conditions, including the maximum applied load of 84.584 N.

4. Conclusions

The finite element simulation demonstrated that the proposed Archimedes screw turbine (AST) casing made of ASTM A36 steel exhibits adequate structural performance under the applied loading conditions. The results confirm that the casing operates within the elastic region and maintains a sufficient safety margin throughout all simulated cases, indicating reliable structural behaviour for micro-hydropower applications. The identified stress and strain concentrations near the casing support and end regions highlight critical areas for future structural optimisation to improve load distribution and minimise localised mechanical effects. From a design perspective, the findings suggest that the proposed casing configuration can provide a stable and mechanically reliable structure for AST systems operating under low-head conditions. Future studies should incorporate dynamic loading, fatigue analysis, and experimental validation to further evaluate long-term structural performance under real operating conditions. Future work should include experimental validation, dynamic loading, fatigue analysis, and water pressure distribution from
CFD, coupled CFD-FEA analysis, weld/joint assessment, and optimisation of casing thickness to avoid overdesign.

Acknowledgements

The authors would like to express their gratitude to all parties who have contributed to the simulation process and to the discussions regarding the simulation results.

References

[1] Suherman *et al.*, "Design and Investigation of Archimedes Screw Turbine: Influence of Inclination Angle on Power Production," in *International Conference on Experimental and Computational Mechanics in Engineering*, 2022, pp. 53-63: Springer.

[2] K. Umurani, A. M. Siregar, and S. Al-Amin, "Pengaruh Jumlah Sudu Prototype Pembangkit Listrik Tenaga Mikrohidro Tipe Whirlpool Terhadap Kinerja," *Jurnal Rekayasa Material, Manufaktur dan Energi,* vol. 3, no. 2, pp. 103-111, 2020.

[3] E. Saefudin, T. Kristyadi, M. Rifki, and S. Arifin, "Turbin screw untuk pembangkit listrik skala mikrohidro ramah lingkungan," *Rekayasa Hijau: Jurnal Teknologi Ramah Lingkungan,* vol. 1, no. 3, 2017.

[4] I. K. Ardika, A. I. Weking, and L. Jasa, "Analisa Pengaruh Jarak Sudu Terhadap Putaran Turbin Ulir Pada Pembangkit Listrik Tenaga Mikro Hidro," *Majalah Ilmiah Teknologi Elektro,* vol. 18, no. 2, pp. 217-226, 2019.

[5] Y. Hizhar, B. Yulistianto, and S. Darmo, "Rancang Bangun dan Studi Eksperimental Pengaruh Perbedaan Jarak Pitch dan Kemiringan Poros terhadap Kinerja Mekanik Model Turbin Ulir 2 Blade Pada Aliran Head Rendah," *METAL: Jurnal Sistem Mekanik dan Termal,* vol. 1, no. 1, pp. 27-34, 2017.

[6] E. Eswanto, S. Siman, M. Pasaribu, S. Suherman, I. Ilmi, and M. Hamidi, "The Phenomenon of Water Fluid Flow Distribution in Hydropower Pico-Hydro Viewed from the Number of Turbine Screw Winding," *Journal of Advanced Research in Fluid Mechanics and Thermal Sciences,* vol. 124, no. 2, pp. 110-123, 2024.

[7] M. A. T. Saputra, A. I. Weking, and I. W. Artawijaya, "Eksperimental Pengaruh Variasi Sudut Ulir Pada Turbin Ulir (Archimedean Screw) Pusat Pembangkit Listrik Tenaga Mikro Hidro Dengan Head Rendah," *Majalah Ilmiah Teknologi Elektro,* vol. 18, no. 1, pp. 83-90, 2019.

[8] S. Dharma, "Simulasi Computational Fluid Dynamic (CFD) Pada Turbin Screw Archimedes Skala Kecil: Simulasi Computational Fluid Dynamic (CFD) Pada Turbin Screw Archimedes Skala Kecil," *ABEC Indonesia,* vol. 9, 2021.

[9] I. G. W. Putra, A. I. Weking, and L. Jasa, "Analisa Pengaruh Tekanan Air Terhadap Kinerja PLTMH dengan Menggunakan Turbin Archimedes Screw," *Majalah Ilmiah Teknologi Elektro,* vol. 17, no. 3, pp. 385-392, 2018.

[10] H. B. Harja, H. Abdurrahim, S. Yoewono, and H. Riyanto, "Penentuan Dimensi Sudu Turbin dan Sudut Kemiringan Poros Turbin pada Turbin Ular Archimedes," *Metal Indonesia,* vol. 36, no. 1, pp. 26-33, 2016.

[11] A. Havendri and H. Lius, "Perancangan dan Realisasi Model Prototipe Turbin Air Type Screw (Archimedean Turbine) untuk Pembangkit Listrik Tenaga Mikrohidro dengan Head Rendah di Indonesia," *Jurnal Teknik,* vol. 31, 2009.

[12] W. Chan, U. Jamaludin, and N. Azahari, "Archimedes Screw Pump Efficiency Based on Three Design Parameters using Computational Fluid Dynamics Software–Ansys CFX," in *Journal of Physics: Conference Series*, 2024, vol. 2688, no. 1, p. 012015: IOP Publishing.

[13] A. Mukesh, R. Rahul, D. Stephen, R. Jose, and A. P. Savio, "Design and analysis of blade parameters in screw turbine to improve efficiency," in *AIP Conference Proceedings*, 2024, vol. 3134, no. 1, p. 070003: AIP Publishing LLC.

[14] R. L. Kazem Shahverdi, JM Maestre, Gholamhassan Najafi "CFD numerical simulation of Archimedes screw turbine with power output analysis," *Ocean Engineering,* vol. 231, pp. 1-8, 2021.

[15] I. Brinas, F. D. Popescu, A. Andras, S. M. Radu, and L. Cojanu, "A computerized analysis of flow parameters for a twin-screw compressor using SolidWorks flow simulation," *Computation,* vol. 13, no. 8, p. 189, 2025.

[16] H. Prasetyo, E. Budiana, D. Tjahjana, and S. Hadi, "The Simulation Study of Horizontal Axis Water Turbine Using Flow Simulation Solidworks Application," in *IOP Conference Series: Materials Science and Engineering*, 2018, vol. 308, no. 1, p. 012022: IOP Publishing.

[17] R. Rahmawaty, S. Suherman, S. Dharma, and A. Sai'in, "Kajian Eksperimental pada Turbin Screw Archimedes Skala Kecil," *Jurnal Rekayasa Mesin,* vol. 17, no. 1, pp. 95-102, 2022.

[18] H. B. Harja, M. Y. Diratama, and R. A. Febriani, "Preliminary Development the Optimum Dimension Estimator and 3D Engineering Drawing Generator of Archimedes Screw Turbine Shaft," in *International Conference on Mechanical Engineering*, 2023, pp. 39-46: Springer.

[19] N. S. Abd Rahim, C. C. Yang, and N. F. N. binti Mamat, "Optimizing an Archimedean Screw Turbine (AST) at Low Water Flow Velocity for Clean Energy Generation," in *International conference on Advancement in Materials, Manufacturing, and Energy Engineering*, 2024, pp. 83-88: Springer.

[20] A. D. Andi Saidah, Rajes Khana and Jili Edo Pratama, "Testing Simulation in the River of Archimedes Screw Turbine on the Cilember River in Bogor Using SolidWorks Software," *Proceedings of the 4th International Seminar and Call for Paper (ISCP UTA '45 JAKARTA),* pp. 399-405, 2023.